

Dear author,

Please note that changes made in the online proofing system will be added to the article before publication but are not reflected in this PDF.

We also ask that this file not be used for submitting corrections.



Contents lists available at ScienceDirect

Mechanics Research Communications

journal homepage: www.elsevier.com/locate/mechrescom

Deformation of atomic models and their equivalent continuum counterparts using Eringen's two-phase local/nonlocal model[☆]

Meral Tuna^{a,*}, Mesut Kirca^a, Patrizia Trovalusci^b

^aFaculty of Mechanical Engineering, Istanbul Technical University, Istanbul, Turkey

^bDepartment of Structural and Geotechnical Engineering, Sapienza University of Rome, Via A. Gramsci, 53, Rome, 00197 Italy

ARTICLE INFO

Article history:

Received 15 December 2018

Revised 20 February 2019

Accepted 6 April 2019

Available online xxx

Keywords:

Two-phase local/nonlocal model

Eringen

Atomic array

Finite element method

ABSTRACT

The aim of this contribution is to formulate equivalent continuum finite element model for two-dimensional atomic arrays under plane-stress condition, based on Eringen's two phase local/nonlocal model. The interaction between the atoms is modelled using translational and rotational linear elastic springs including both nearest and second nearest neighbor relations. Explicit relations between those set of springs and material properties of associated continuum model is looked for by means of equivalency of potential energy stored in atomic bonds and strain energy of continuum. Possibility of reducing computational burden of full atomic models by equivalent continuum models is discussed. This study may be regarded as the first step in composing a partitioned-domain multiscale model; with possibly smoother transition between coarse and fine scales due to the ability of nonlocal continuum model in incorporating long-range interactions.

© 2019 Published by Elsevier Ltd.

1. Introduction

In recent years, continuum theories, capable of including the size effects, have gained considerable attention of researchers for the investigation of nano and micro sized structures. Among them, Eringen's constitutive model is one of the most widely used non-local theories, as it incorporates a small-scale parameter into the constitutive equation to capture micro/nano structural effects in continuous media [1–4]. It is originally formulated in an integral form, and simplified to a differential counterpart; yet, due to paradoxical outcomes of the latter for certain mechanical problems [5–7], the former form has also been substantially used [8–13].

This study concentrates on integral form of Eringen's two-phase local/nonlocal model [14] to investigate the behaviour of specific discrete systems. In fact, linking discrete systems to continuum approaches dates back to early molecular models of 19th century, through which the first attempts to derive the constitutive equations of continua was initiated [15,16]. These approaches are still quite promising in adopting discrete to scale dependent continuous models [17–19]. Here, particularly simple discrete system: 1-

D atomic chain and 2-D atomic array models are considered. Interatomic potentials are modelled using linear elastic translational and rotational springs, for both the nearest, and second nearest neighbor relations from which the nonlocality arises. A linear system of equations for the atomic models are derived by means of the principle of minimum total potential. Finite element formulation of continuum is developed for bar and plane stress problems, which paves the way to look for equivalent models by linking the strain energy on the continuum level to the energy stored in atomic bonds, assuming uniform deformation field [20–23], for 1-D and 2-D atomic structures, respectively. Indeed, explicit relations of material properties are obtained; albeit some of which require numerical integration schemes. Their equivalency are tested by examining same mechanical problem with both approaches. Despite some studies focusing on only translational springs and local elasticity [24,25], to the best of authors's knowledge this study is the first attempt to provide the closed-form expressions for non-local material properties in terms of spring constants introducing all possible interatomic relations. It is thought that the results provided herein are encouraging for the possibility of modelling transition zones of partitioned-domain multiscale models; as they indicate that Eringen's two phase model can capture the displacements of atomic arrays once the material properties ensuring energy equivalency are used.

[☆] This work was done when Meral Tuna was Visiting Researcher at DISG, Sapienza University of Rome, the support of which is gratefully acknowledged. The authors wish to thank Ugurcan Eroglu, visiting researcher at Sapienza University of Rome, for his assistance on formatting the manuscript.

* Corresponding author.

E-mail address: tunamer@itu.edu.tr (M. Tuna).

44 **2. Material and methods**

45 In this section, derivation of governing equation for static prob-
 46 lems of 1-D atomic chain and 2-D atomic arrays, and FEM formula-
 47 tion of continuum with Eringen's two-phase local/nonlocal consti-
 48 tutive relation are presented. Distribution of the atoms/nodes are
 49 considered to be uniform throughout the axes. The nodes and the
 50 atoms in continuum and atomic models, respectively, do not nec-
 51 essarily need to be coincident. In fact, it is aimed to discretize the
 52 continuum models by using very coarse mesh in order to high-
 53 light its superiority in terms of computational cost. Materials in the
 54 continuum models are assumed to be linear, elastic and isotropic,
 55 in agreement with the atomic models which consist of identical
 56 atoms connected via linear elastic springs. Small deformations and
 57 displacements of all structures are considered; hence, linear mod-
 58 els are used. For calculations, an in-house code is developed.

59 **2.1. One-dimensional case**

60 In 1-D case, both atomic and continuum models has one degree
 61 of freedom: translation in longitudinal axis x . In fact, it may not
 62 be of interest in practical applications; however, it is intended to
 63 examine them for the validation of present approach and integrity.

64 **2.1.1. Atomic chain**

65 1-D atomic chain model is composed by equally spaced (with
 66 a distance of l_a), identical atoms. Interatomic potential is repre-
 67 sented using linear elastic translational springs representing both
 68 the nearest (k_1) and the second nearest (k_2) neighbor relations. En-
 69 ergy of i th atom (i.e. \mathcal{E}_i^{atom}) with displacement of u_i can be written
 70 as follows:

$$\mathcal{E}_i^{atom} = \frac{k_1}{4} [(u_{i+1} - u_i)^2 + (u_i - u_{i-1})^2] + \frac{k_2}{4} [(u_{i+2} - u_i)^2 + (u_i - u_{i-2})^2] \quad (1)$$

71 **Remark 1.** Eq. (1) is valid only for the atoms located at least $2l_a$
 72 away from the boundaries for our case in which interactions of
 73 atoms up to their second neighbors are taken into account. Hence,
 74 Eq. (1) must be simplified for the boundary atoms regarding the
 75 non-existing bonds.

76 Consequently, the internal energy of the atomic chain consisting
 77 of N atoms can be expressed as

$$\mathcal{E}_{int}^a = \sum_{i=1}^N \mathcal{E}_i^{atom} \quad (2)$$

78 Each atom must be in equilibrium under the internal forces,
 79 $(f_i)_{int}$, and external forces, $(f_i)_{ext}$:

$$(f_i)_{int} + (f_i)_{ext} = 0, \quad (f_i)_{int} = -\frac{\partial \mathcal{E}_{int}^a}{\partial u_i} = -\frac{\partial (\mathcal{E}_{i-2}^a + \mathcal{E}_i^a + \mathcal{E}_{i+1}^a + \mathcal{E}_{i+2}^a)}{\partial u_i} \quad (3)$$

80 (3) provides a formulation similar to classical FEM:

$$\mathbf{K}_a \mathbf{d}_a = \mathbf{f}_a \quad (4)$$

81 where \mathbf{f}_a , \mathbf{d}_a and \mathbf{K}_a refer to external force vector, displacement
 82 vector, and the stiffness matrix, respectively.

83 **2.1.2. Continuum model**

84 From continuum mechanics point of view, 1-D atomic chain can
 85 be modelled as a bar structure characterized by a total length L ,
 86 cross-sectional area, A , elasticity modulus E , and a material param-
 87 eter κ providing the nonlocal small-size effects through a kernel

function, $\tau(r, \kappa)$. For a bar along a horizontal axis $x \in [0, L]$, the
 constitutive relation of Eringen's two-phase local/nonlocal model
 is,

$$\sigma_x = \lambda D \varepsilon_x(x) + \psi \int_0^L \tau(|x - \bar{x}|, \kappa) D \varepsilon_x(\bar{x}) d\bar{x} \quad (5)$$

where σ_x and ε_x keep their usual definitions of normal stress and
 strain. The weights of the local and nonlocal parts are regulated
 through a fraction coefficient, $\lambda \in [0, 1]$, and $\psi = 1 - \lambda$. $\lambda = 0$ and
 $\lambda = 1$ induce full nonlocal and full local models, respectively. Be-
 ing different from local elasticity, in nonlocal models, stress at a
 point is linked to the strain of the entire domain through a kernel
 function, which is assumed bi-exponential

$$\tau(r, \kappa) = e^{-\frac{r}{\kappa}} / (2\pi^{n-1} \kappa^n) \quad (6)$$

n being the dimension of the structure. Other kernel functions
 to represent nonlocal effects are also available [26].

In natural coordinate system $\zeta = (l_c + 2x - 2x_2)/l_c$, displace-
 ment field may be approximated by two-noded linear bar elements
 with equal length, l_c .

$$\mathbf{u}_e(\zeta) = \mathbf{N} \mathbf{d}_e, \quad \mathbf{N}(\zeta) = \begin{bmatrix} \frac{(1-\zeta)}{2} & \frac{(1+\zeta)}{2} \end{bmatrix}$$

$$\mathbf{d}_e = \{d_{1x} \ d_{2x}\}_e^T, \quad \varepsilon_e = \mathbf{B}_e \mathbf{d}_e$$

$$\mathbf{B}_e = \frac{\partial \mathbf{N}(\zeta)}{\partial \zeta} \frac{\partial \zeta}{\partial x} = \begin{bmatrix} -\frac{1}{2} & \frac{1}{2} \end{bmatrix} \mathbf{J}_e^{-1} \quad (7)$$

with d_{1x} and d_{2x} being longitudinal displacement of the 1st and
 the 2nd node, and ε_e the strain of element e . With those defini-
 tions at hand, strain energy of the bar,

$$U = \frac{1}{2} \int_V \varepsilon(x) \sigma(x) dV(x) \quad (8)$$

With $L_{mm} = \mathbf{d}_m^T \mathbf{B}_m^T E_n \mathbf{B}_n \mathbf{d}_n$, it may be approximated, by using M
 uniform elements, as

$$U_{FEM} = \frac{A}{2} \left(\lambda \sum_{m=1}^M \int_{-1}^1 L_{mm} \det |\mathbf{J}_m| d\zeta + \psi \sum_{m=1}^M \sum_{n=1}^M \int_{-1}^1 \int_{-1}^1 \frac{e^{-\frac{|\zeta-\bar{\zeta}|}{2\kappa}}}{2\kappa} L_{mn} \det |\mathbf{J}_n| \det |\mathbf{J}_m| d\bar{\zeta} d\zeta \right) \quad (9)$$

Total potential, Π , can be written in terms of strain energy with
 FEM approach, U_{FEM} , plus external work potential, W_{FEM} , and must
 be minimum for equilibrium; hence,

$$\Pi = U_{FEM} + W_{FEM}, \quad \frac{\partial \Pi}{\partial \mathbf{d}_i} = 0, \quad (i = 1, 2, \dots, M) \quad (10)$$

which requires, \mathbf{d} being the global displacement vector. Then, in-
 serting (7) into (10)₂ provides

$$\mathbf{f}_m = \lambda \mathbf{k}_m \mathbf{d}_m + \psi \mathbf{k}_{mm} \mathbf{d}_m + 2\psi \sum_{n=1, n \neq m}^M \mathbf{k}_{mn} \mathbf{d}_n$$

$$\mathbf{k}_m = \frac{EA}{l_c} \begin{bmatrix} 1 & -1 \\ -1 & 1 \end{bmatrix}$$

$$\mathbf{k}_{mm} = \frac{EA(l_c + \kappa(e^{-\frac{l_c}{\kappa}} - 1))}{l_c^2} \begin{bmatrix} 1 & -1 \\ -1 & 1 \end{bmatrix}$$

$$\mathbf{k}_{mn} = \frac{\kappa EA e^{-\frac{(|m-n|+1)l_c}{\kappa}} (e^{\frac{l_c}{\kappa}} - 1)^2}{4l_c^2} \begin{bmatrix} 1 & -1 \\ -1 & 1 \end{bmatrix} \quad (11)$$

\mathbf{k}_{mm} , stands for the contribution of the m th element to its own
 energy, while \mathbf{k}_{mn} and \mathbf{k}_{nm} account for the influence exerted on
 the m th element by the remaining elements, and the influence ex-
 erted by the m th element to the other elements. Also, it is vital to

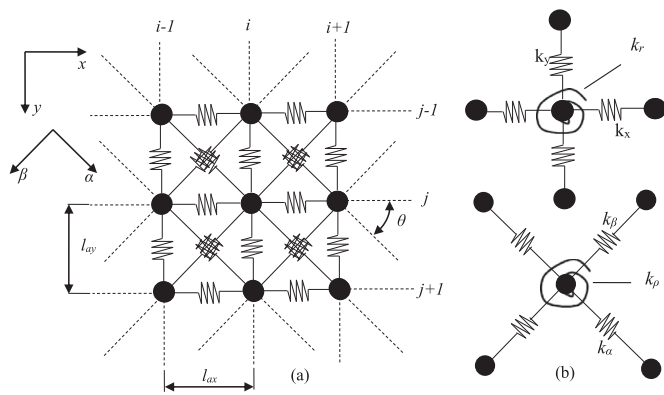


Fig. 1. Illustration of 2-D atomic array model.

point out that $\mathbf{k}_{mn} = \mathbf{k}_{nm}^T$ in case of homogeneous material properties. Consequently, global form of the stiffness matrix including all degrees of freedom is constructed through proper assemblage of the element stiffness matrices. Based on the minimum potential energy principle, global form of finite element formulation can be represented as:

$$\mathbf{K}_c \mathbf{d}_c = \mathbf{f}_c \quad (12)$$

where \mathbf{f}_c and \mathbf{d}_c are external force and displacement vector, respectively, and \mathbf{K}_c is called as the global stiffness matrix with a dimension of $(M + 1) \times (M + 1)$. To validate FE model, the results are compared with the analytical expressions given in [27] for the same boundary conditions. Although slight differences at the boundaries due to different solution techniques, a very good agreement is achieved.

Finally, regarding the energy equivalency for the uniform deformation field of atomic and continuum models, following relation between the material properties and the spring constants is obtained.

$$k_1 + 4k_2 = \frac{EA}{l_a} \left[\psi \left(1 + \frac{\kappa}{l_c} g(zn) \right) + \lambda \right] \quad (13)$$

$$g(zn) = \left(e^{-\frac{(zn+1)l_c}{\kappa}} - e^{-\frac{zn l_c}{\kappa}} \right)$$

where zn refers to the total number of elements that fall in the radius of influence zone of an element. Hence, its value should be increased with the nonlocality.

2.2. Two-dimensional case

To parameterize the position of points, components of forces and displacements, etc., a Cartesian coordinate system x, y with unit vectors $\mathbf{e}_1, \mathbf{e}_2$ are used. In 2-D case, atomic and continuum models possess two translational degree of freedoms: planar displacements, u and v ; the components of displacement vector \mathbf{u} .

2.2.1. Atomic array

In the present study, a square 2-D atomic array model is composed using equally spaced (i.e. $l_{ax} = l_{ay} = l_a$), identical atoms as illustrated in Fig. 1a. Linear elastic translational and rotational springs for the nearest and the second nearest neighbor relations are utilized to represent the atomic interactions. The translational springs with constants $k_x, k_y, k_\alpha, k_\beta$, are oriented along x, y, α and β directions, respectively, while the rotational springs with constants k_r and k_ρ connect the atoms positioned along $x - y$ and $\alpha - \beta$ axes, accordingly (see Fig. 1b).

The internal energy can be expressed in terms of bond length and bond angle variations by specifying each contribution individually. For brevity, instead of the energy of the atom, contribution

of the rotational springs located at the j th row and i th column of the array is given below:

$$(\mathcal{E}_{ji}^{bond})_{rot} = \sum_{n=1}^2 \left\{ \frac{k_{r_n}}{2} \left[\left(\frac{u_{j+n,i} - u_{j,i}}{l_{ay}} + \frac{v_{j,i} - v_{j,i-n}}{l_{ax}} \right)^2 + \left(\frac{u_{j-n,i} - u_{j,i}}{l_{ay}} + \frac{v_{j,i-n} - v_{j,i}}{l_{ax}} \right)^2 + \left(\frac{u_{j,i} - u_{j+n,i}}{l_{ay}} + \frac{v_{j,i} - v_{j,i+n}}{l_{ax}} \right)^2 + \left(\frac{u_{j,i} - u_{j-n,i}}{l_{ay}} + \frac{v_{j,i+n} - v_{j,i}}{l_{ax}} \right)^2 \right] \right\} \quad (14)$$

$$+ \frac{k_{\rho_n}}{2\ell^2} \left\{ \left[\left(\{u_{j,i} - u_{j+n,i-n} + v_{j,i} - v_{j+n,i+n}\}c + \{u_{j+n,i+n} - u_{j,i} + v_{j,i} - v_{j+n,i-n}\}s \right)^2 + \left(\{u_{j+n,i-n} - u_{j,i} + v_{j,i} - v_{j-n,i-n}\}c + \{u_{j-n,i-n} - u_{j,i} + v_{j+n,i-n} - v_{j,i}\}s \right)^2 + \left(\{u_{j,i} - u_{j-n,i+n} + v_{j+n,i+n} - v_{j,i}\}c + \{u_{j,i} - u_{j+n,i+n} + v_{j,i} - v_{j-n,i+n}\}s \right)^2 + \left(\{u_{j-n,i+n} - u_{j,i} + v_{j-n,i-n} - v_{j,i}\}c + \{u_{j,i} - u_{j-n,i-n} + v_{j-n,i+n} - v_{j,i}\}s \right)^2 \right] \right\}$$

where s and c are $\sin \theta$ and $\cos \theta$, respectively, the subscripts 1 and 2 of k correspond to the nearest and second-nearest relations, and $\ell^2 = l_{ax}^2 + l_{ay}^2$. Energy of an atom due to translations is

$$(\mathcal{E}_{j,i}^{atom})_{str} = \sum_{n=1}^2 \left\{ \frac{k_{x_n}}{4} \left[(u_{j,i+n} - u_{j,i})^2 + (u_{j,i} - u_{j,i-n})^2 \right] + \frac{k_{y_n}}{4} \left[(v_{j+n,i} - v_{j,i})^2 + (v_{j,i} - v_{j-n,i})^2 \right] + \frac{k_{\alpha_n}}{4} \left[\left(\{u_{j+n,i+n} - u_{j,i}\}c + \{v_{j+n,i+n} - v_{j,i}\}s \right)^2 + \left(\{u_{j,i} - u_{j-n,i-n}\}c + \{v_{j,i} - v_{j-n,i-n}\}s \right)^2 \right] + \frac{k_{\beta_n}}{4} \left[\left(\{u_{j,i} - u_{j+n,i-n}\}s + \{v_{j+n,i-n} - v_{j,i}\}c \right)^2 + \left(\{u_{j-n,i+n} - u_{j,i}\}s + \{v_{j,i} - v_{j-n,i+n}\}c \right)^2 \right] \right\} \quad (15)$$

Eventually, total internal energy of a 2-D array of N atoms, is calculated as follows.

$$\mathcal{E}_{int}^a = \sum_{j=1}^N \sum_{i=1}^N (\mathcal{E}_{j,i}^{atom})_{str} + \sum_{j=1}^N \sum_{i=1}^N (\mathcal{E}_{j,i}^{bond})_{rot} \quad (16)$$

Note that the expressions given in Eqs. (14) and (15) are valid only for the atoms and the bonds located sufficiently away from the boundaries. For the others, some simplifications are required to avoid miscalculation.

Equilibrium condition of 2-D array requires

$$(\mathbf{f}_i)_{int} + (\mathbf{f}_i)_{ext} = 0, \quad (\mathbf{f}_i)_{int} = - \frac{\partial \mathcal{E}_{int}^a}{\partial \mathbf{u}_i} \quad (17)$$

which may be represented in an identical form to (4), where the components of stiffness matrix are given as,

$$K_{2i-1,2j-1} = \frac{\partial \mathcal{E}_{int}^a}{\partial u_i \partial u_j}, \quad K_{2i,2j} = \frac{\partial \mathcal{E}_{int}^a}{\partial v_i \partial v_j} \quad (18)$$

2.2.2. Continuum model

From the view of continuum mechanics, 2-D atomic array can be modelled a continuum occupying 2-D planar region. Constitu-

tive relation is similar to what is assumed in 1-D case:

$$\sigma(x, y) = \lambda \mathbf{C} : \boldsymbol{\varepsilon}(x, y) + \psi \iint \tau(r, \kappa) \mathbf{C} : \boldsymbol{\varepsilon}(\bar{x}, \bar{y}) d\bar{A} \quad (19)$$

where, in case of plane-stress condition,

$$\sigma(x, y) = \begin{Bmatrix} \sigma_{xx} \\ \sigma_{yy} \\ \sigma_{xy} \end{Bmatrix}, \quad \boldsymbol{\varepsilon}(x, y) = \begin{Bmatrix} \varepsilon_{xx} \\ \varepsilon_{yy} \\ 2\varepsilon_{xy} \end{Bmatrix}, \quad (20)$$

$$\mathbf{C} = \frac{E}{(1-\nu^2)} \begin{bmatrix} 1 & \nu & 0 \\ \nu & 1 & 0 \\ 0 & 0 & \frac{(1-\nu)}{2} \end{bmatrix}$$

$d\bar{A}$ is equal to $d\bar{x}d\bar{y}$, differential area element. Kernel function $\tau(r, \kappa)$ is given in (6), obviously for $n = 2$ [28], and r is the Euclidean distance between the point of interest and its neighbor points.

For finite element (FE) approximation to displacement and strain fields within an element e ; \mathbf{u}_e and $\boldsymbol{\varepsilon}_e$, discretization with 4-noded linear elements with bilinear shape functions (i.e. \mathbf{N}) are used. In a natural coordinate system:

$$\mathbf{u}_e(\zeta, \eta) = N(\zeta, \eta) \mathbf{d}_e$$

$$\boldsymbol{\varepsilon}_e = \mathbf{L}_e \mathbf{N} \mathbf{d}_e = \mathbf{B}_e \mathbf{d}_e$$

$$\mathbf{L}_e = \begin{bmatrix} \frac{\partial}{\partial x} & 0 \\ 0 & \frac{\partial}{\partial y} \\ \frac{\partial}{\partial y} & \frac{\partial}{\partial x} \end{bmatrix}, \quad \mathbf{J} = \frac{1}{2} \begin{bmatrix} l_{cx} & 0 \\ 0 & l_{cy} \end{bmatrix} \quad (21)$$

The strain energy of a plate with thickness h is known as,

$$U = \frac{h}{2} \left(\lambda \iint \boldsymbol{\varepsilon}(x, y)^T \mathbf{C} \boldsymbol{\varepsilon}(x, y) dA + \psi \iint \iint \tau(r, \kappa) \boldsymbol{\varepsilon}^T(x, y) \bar{\mathbf{C}} \boldsymbol{\varepsilon}(\bar{x}, \bar{y}) d\bar{A} dA \right) \quad (22)$$

Then, the principle of minimum total potential, similar to what is done in 1-D case, provides the FE formulation of 2-D continua,

$$\mathbf{f}_m = \lambda \mathbf{k}_m \mathbf{d}_m + \psi \mathbf{k}_{mm} \mathbf{d}_m + 2\psi \sum_{n=1, n \neq m}^M \mathbf{k}_{mn} \mathbf{d}_n,$$

$$\mathbf{k}_m = h \int_{-1}^1 \int_{-1}^1 \mathbf{B}_m^T(\zeta, \eta) \mathbf{C}_m \mathbf{B}_m(\zeta, \eta) \det |\mathbf{J}_m| d\zeta d\eta,$$

$$\mathbf{k}_{mn} = \frac{h}{2} \int_{-1}^1 \int_{-1}^1 \int_{-1}^1 \int_{-1}^1 \tau(r, \kappa) \mathbf{A}_{mn} d\bar{\zeta} d\bar{\eta} d\zeta d\eta,$$

$$r = \sqrt{(\zeta - \bar{\zeta})^2 + (\eta - \bar{\eta})^2},$$

$$\mathbf{A}_{mn} = \mathbf{B}_m^T(\zeta, \eta) \mathbf{C}_n \mathbf{B}_n(\bar{\zeta}, \bar{\eta}) \det |\bar{\mathbf{J}}_n| \det |\mathbf{J}_m|. \quad (23)$$

In terms of global force vector \mathbf{f}_c , global displacement vector \mathbf{d}_c and global stiffness matrix \mathbf{K}_c , an identical representation of (23) to (12) is possible.

Remark 2. The integration operations of the nonlocal part are performed using Gauss Quadrature (GQ) method. The number of GQ points should be increased depending on the ratio between the nonlocal parameter and the element length (i.e. κ/l_{cx} or κ/l_{cy}), and the calculated part of the stiffness matrix (i.e. k_{mm} or k_{mn}).

Despite its capabilities, integral form of nonlocal theory based FEM formulation has been only conducted by a limited number of researchers, such as [29–31]. For the validation of the FE model, the results are compared with the ones given in [30] considering the same boundary conditions. Slight differences in the strain field

Table 1
Material properties.

case	λ	κ [nm]
1	1	any value
2	0.2	0.025 L
3	0.2	0.050 L
4	0.7	0.050 L

is encountered only at the boundaries of the domain due to different element types: in the reference article 8-noded Serendipity element is used, while in the present study the formulation is derived based on the 4-noded linear elements. In order to obtain material properties in terms of spring constants (i.e. E and κ), the total energy of the unit cell in the atomic model and the total energy of the corresponding element in the continuum model are compared under uniform deformation fields such as; uniaxial, biaxial, pure shear and simple shear. Considering isotropy,

$$k_x = k_y = k_l, \quad k_\alpha = k_\beta = k_s, \quad G = \frac{E}{2(1+\nu)} \quad (24)$$

following expressions are obtained:

$$E = \frac{1}{\lambda + \psi \xi} \frac{(k_{E_1} + 2k_{E_2})(8k_{E_3} + k_{E_1} l_a^2)}{h(4k_{E_3} + (k_{E_1} + k_{E_2}) l_a^2)}$$

$$\nu = \frac{-4k_{E_3} + k_{E_2} l_a^2}{4k_{E_3} + (k_{E_1} + 2k_{E_2}) l_a^2}, \quad G = \frac{1}{\lambda + \psi \xi} \frac{4k_{E_4} + k_{E_2} l_a^2}{h l_a^2},$$

$$k_r = k_\rho + \left(\frac{k_l}{8} - \frac{k_s}{4} \right) l_a^2$$

$$k_{E_1} = k_{l_1} + 4k_{l_2}, \quad k_{E_2} = k_{s_1} + 4k_{s_2},$$

$$k_{E_3} = k_{\rho_1} + 4k_{\rho_2}, \quad k_{E_4} = k_{r_1} + 4k_{r_2}, \quad (25)$$

with ξ , which varies with the value of the nonlocal parameter, being basically a constant arising from numerical integration; hence, it depends on zn and the number of GQ points. An explicit expression for ξ is possible, but too long to be reported within the length of this article.

3. Numerical examples

In this section, static response of atomic and continuum models are examined for some benchmark problems of practical importance.

3.1. One-dimensional case

An atomic chain of $L = 1$ [nm] length, which is thought of consisting 161 atoms, is investigated as an example. 20 finite elements are used to construct its approximated continuum model. The spring constants stimulating the interaction with the nearest and the second nearest neighbor atoms are assumed equal: $k_1 = k_2 = 80$ [nN/nm]. Young's modulus is calculated by Eq. (25), assuming $A = 1$ [nm²]. The structure is investigated under both constant and linearly varying normal force, which may be due to a tip point load, $f = 1$ nN, and uniformly distributed load $q = f/L$. Material properties are provided in Table 1. Number of elements inside the radius of influence zone, zn , is set to 9 considering highest $\kappa = 0.05L$ [nm]. Assuming a fixed mid-point, axial displacement fields of atomic and equivalent continuum models are plotted in Fig. 2, where an excellent agreement is achieved for all cases. Only appreciable discrepancy is apparent for uniform strain field around boundaries of the domain; see Fig. 2a. This is due to the phenomenon known as *boundary effect*, as also pointed out by Remark 1. However, it also depends on the state of stress around the corresponding boundary domain. This is also evidenced by

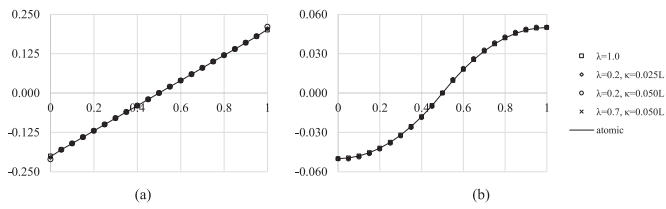


Fig. 2. Displacement values at atoms/nodes under (a) tip point load f , and (b) equally distributed axial load, q . x and y axis denote coordinate x [nm] and axial displacement u [nm], respectively.

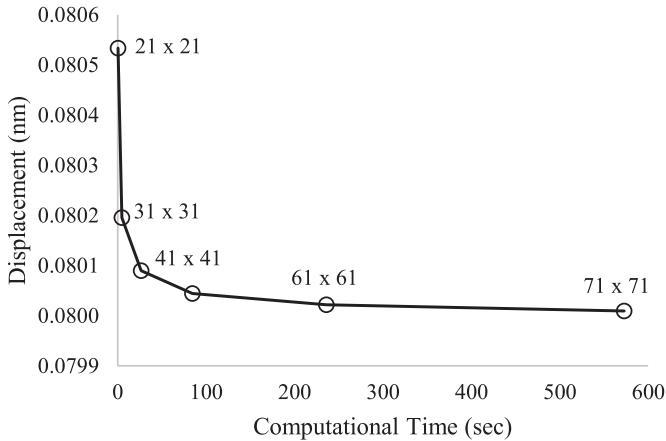


Fig. 3. The variation of $u(40 \text{ nm}, 50 \text{ nm})$ and computational time with respect to total number of atoms.

239 deformation field of uniformly distributed load in which case, a
 240 perfect correspondence between displacement is achieved, as il-
 241 lustrated at Fig 2 b. Nevertheless, minimizing such a discrepancy
 242 looks possible by proper selection of nonlocal material parameters.

243 3.2. Two-dimensional case

244 For 2-D case, an evenly spaced atomic array occupying a square
 245 region with edge length $L = 100$ [nm] is considered. Continuum
 246 approximation of it consists of 21×21 nodes, while different num-
 247 ber of atoms are considered. Similar to 1-D problem, spring con-
 248 stants are assumed equal.

249 There are two important points to be stressed out:
 250 (1) Spring constants can be arbitrarily determined as long as
 251 they satisfy Eqs. (24) and (25)₄.

252 (2) Different values of spring constants may yield same material
 253 properties as clearly seen from Eq. (25).

254 Regarding these facts, although an infinite number of al-
 255 ternatives exists, only the followings are considered: $k_t = 1.5$
 256 [nN/nm], $k_s = 0.91667$ [nN/nm], $k_\rho = 0.0625l_a^2$ [nN.nm] and $k_r =$
 257 $0.0208333l_a^2$ [nN.nm]. Numerical experiments showed that consid-
 258 eration of different values for spring constants yield practically
 259 identical deformation fields as the number of atoms are increased.
 260 However, for the sake of brevity, results of those numerical exper-
 261 iments paving the way to this conclusion are not reported here.

262 As a first step, the deformation fields of the atomic array with
 263 different number of atoms are investigated. Fig. 3 shows the dis-
 264 placement along x -axis at a point and the computational time re-
 265 quired, for the different number of atoms, in case of uniaxial load-
 266 ing. In the light of Fig. 3, 61×61 number of atoms looks to be an
 267 optimum choice considering the convergence and computational
 268 burden.

269 For continuum model, material properties are listed in Table 1.
 270 Poisson's ratio is calculated as 0.25 for all cases as it does not
 271 depend on either nonlocal parameter or fraction coefficient, while

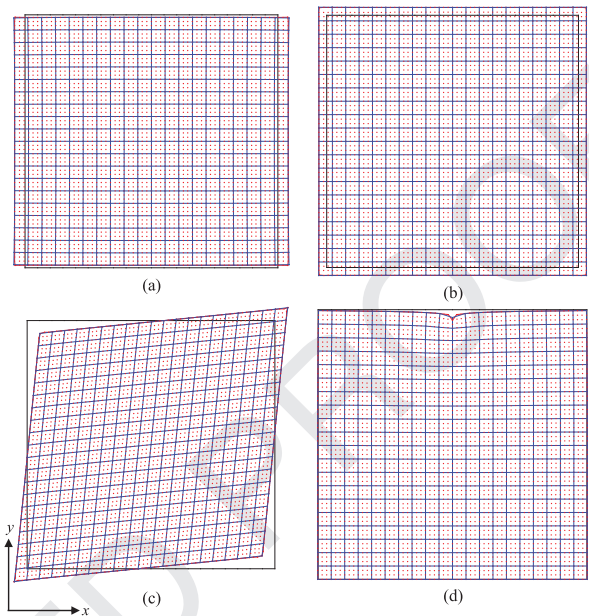


Fig. 4. Deformed configurations of atomic (red), and continuum (blue) models under (a) uniaxial, (b) biaxial, (c) pure shear, and (d) point load conditions. (Black: undeformed configuration) (For interpretation of the references to colour in this figure legend, the reader is referred to the web version of this article.)

Young's modulus is obtained assuming $h = 1$ [nm]. Following load- 272
 ing cases are investigated: 273

(a) constant distributed uniaxial load :

$$q_x(0, y) = -q_x(L, y) = -f/L,$$

(b) constant distributed biaxial load :

$$q_x(0, y) = q_y(x, 0) = -f/L,$$

$$q_x(L, y) = q_y(x, L) = f/L$$

(c) constant distributed shear load :

$$q_x(x, 0) = f/L, q_x(x, L) = -f/L,$$

$$q_y(0, y) = f/L, q_y(L, y) = -f/L$$

(d) point load applied to midpoint of upper edge :

$$f_p(L/2, L) = -f/10,$$

where $f = 100$ [nN]. For the first three loading conditions, the center 274
 point of the domain is assumed fixed. For the last one, the 275
 displacement of atoms/nodes located at the bottom edge are re- 276
 stricted along y direction only. 277

Mechanical problems considered in cases (a)–(c) are basically 278
 simple benchmark problems providing uniform strain fields. On the 279
 other hand, case (d) may be regarded as a coarse approximation to 280
 half infinite continuum under point load, also known as *Flamant* 281
problem. It is simply examined to test the equivalent models wide 282
 range of deformation gradients to see its capability. 283

The deformed configurations of the atomic and continuum 284
 models with $\kappa = 0.050L$ and $\lambda = 0.7$ are illustrated in Fig. 4. At 285
 the first glance, a very good agreement in terms of the displacements 286
 are observed. More in detail, slight difference at boundaries, which 287
 are even more pronounced for corner points, are observed due to 288
 the discrete nature of atomic model, in addition to what is said 289
 for 1-D case. Obviously, including additional connections between 290
 atoms and/or considering different distributions of them will en- 291
 rich the atomic model, which will eventually lead to a more similar 292
 behavior. Displacement fields for the first three loading cases ex- 293
 hibit a similar trend to atomic chain with tip point load, while case 294
 (d) deserves more attention. Vertical displacement of nodes/atoms 295
 at $y = L/4, 3L/4$ are illustrated explicitly at Fig. 5. As the deforma- 296

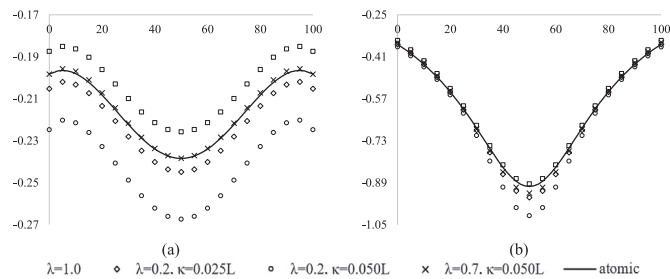


Fig. 5. Displacement values of atoms/nodes located at (a) $y = L/4$ (b) $y = 3L/4$ for case (d). x and y axis denote coordinate x [nm] and vertical displacement v [nm], respectively.

Table 2

Comparison of internal energies [nN.nm] of discrete, local continuum and nonlocal continuum models for 2-D problems.

	(a)	(b)	(c)	(d)
atomic	823.6	1241.8	2116.5	39.443
case 1	800.0	1200.0	2000.0	24.616
case 4	832.1	1247.8	2081.0	29.014

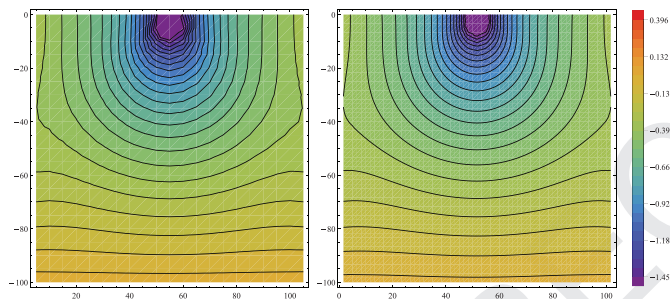


Fig. 6. Contour plots of vertical deformation fields for case (d). *Left:* Nonlocal continuum model (Case 4). *Right:* Atomic model.

tion gradients are appreciable, displacements of equivalent continuum models do not overlap with each other for arbitrary selection of material properties. On the other hand, suitable selection of them (e.g. $\lambda = 0.7$, and $\kappa = 0.05L$) may provide a good match in terms of not only displacement fields, but also total internal energy (see Table 2). Another important interpretation of Fig. 5 may be the following: as Eringen's constitutive relation may be tailored to match atomic displacements, it may also be used in partitioned-domain multiscale models where a strong or weak compatibility of displacement field atomic and continuum models are looked for. The coherence between models are also pointed out through comparing the contour plots illustrated in Fig. 6, for case (d). As an inevitable outcome of finer discretization, the vertical displacement field of atomic model is slightly smoother than its continuum approximation.

4. Conclusion

Present study deals with equivalent continuum finite element models of 2-D atomic array based on Eringen's two phase local/nonlocal model. To have physically reasonable continuum approximation to atomic model, material properties of the former are obtained in closed-form, admitting an energy equivalency under uniform deformation. The advantage and capability of equivalent continuum nonlocal model are highlighted in terms of both accuracy and computational expense via comparing models under various loading scenarios. Numerical experiments show that even though the total number of degree of freedoms is reduced by 90%,

all continuum models are well capable of providing very accurate solutions, while it becomes dependent on nonlocal material parameters for increasing deformation gradients. Such a behaviour is expected due to analogous nature of nonlocal and atomic models, which may help recovering more accurate solutions. This could be further investigated by focusing on entire domain in case of general deformation fields, and might lead to additional constraints on nonlocal material properties, even to unique determination of them. Nevertheless, via exploiting the capability of continuum models including nonlocal effects, a smoother transition between atomic and continuum regions of a partitioned-domain multi-scale model is expected, which is the scope on an ongoing project.

Supplementary material

Supplementary material associated with this article can be found, in the online version, at doi:10.1016/j.mechrescom.2019.04.004.

References

- J. Peddieson, G.R. Buchanan, R.P. McNitt, Application of nonlocal continuum models to nanotechnology, *Int. J. Eng. Sci.* 41 (2003) 305–312.
- C. Polizzotto, Nonlocal elasticity and related variational principles, *Int. J. Solids Struct.* 38 (2001) 7359–7380.
- J.N. Reddy, Nonlocal theories for bending, buckling and vibration of beams, *Int. J. Eng. Sci.* 45 (2007) 288–307.
- J.K. Phadikar, S.C. Pradhan, Variational formulation and finite element analysis for nonlocal elastic nanobeams and nanoplates, *Comput. Mater. Sci.* 49 (2010) 492–499.
- N. Challamel, C.M. Wang, The small length scale effect for a non-local cantilever beam: a paradox solved, *Nanotechnology* 19 (2008) 345703(7).
- J. Fernández-Sáez, R. Zaera, J.A. Loya, J.N. Reddy, Bending of euler-bernoulli beams using Eringen's integral formulation: a paradox resolved, *Int. J. Eng. Sci.* 99 (2016) 107–116.
- C. Li, L. Yao, W. Chen, S. Li, Comments on nonlocal effects in nano-cantilever beams, *Int. J. Eng. Sci.* 87 (2015) 47–57.
- M. Tuna, M. Kirca, Exact solution of Eringen's nonlocal integral model for vibration and buckling of euler-bernoulli beam, *Int. J. Eng. Sci.* 107 (2016) 54–67.
- M. Tuna, M. Kirca, Exact solution of Eringen's nonlocal integral model for bending of Eulerbernoulli and timoshenko beams, *Int. J. Eng. Sci.* 105 (2016) 80–92.
- J. Fernández-Sáez, R. Zaera, Vibrations of Bernoulli-euler beams using the two-phase nonlocal elasticity theory, *Int. J. Eng. Sci.* 119 (2017) 232–248.
- X. Zhu, W. Yuanbin, D. Hui-Hui, Buckling analysis of Euler-Bernoulli beams using Eringen's two-phase nonlocal model, *Int. J. Eng. Sci.* 116 (2017) 130–140.
- H.M. Numanoglu, B. Akgoz, O. Civalek, On dynamic analysis of nanorods, *Int. J. Eng. Sci.* 130 (2018) 33–50.
- C. Polizzotto, P. Fuschi, A. Pisano, A nonhomogeneous nonlocal elasticity model, *Eur. J. Mech.* 25 (2) (2006) 308–333.
- A.C. Eringen, Theory of nonlocal elasticity and some applications, *Res. Mechanica* 21 (1987) 313–342.
- P. Trovalusci, G. Capecchi, G. Ruta, Genesis of the multiscale approach for materials with microstructure, *Arch. Appl. Mech.* 79 (11) (2008) 981.
- D. Capecchi, G. Ruta, P. Trovalusci, Voigt and poincaré's mechanistic-energetic approaches to linear elasticity and suggestions for multiscale modelling, *Arch. Appl. Mech.* 81 (11) (2011) 1573–1584.
- P. Trovalusci, *Molecular Approaches for Multifield Continua: Origins and Current Developments*, Springer, Vienna, pp. 211–278.
- P. Trovalusci, A. Pau, Derivation of microstructured continua from lattice systems via principle of virtual works: the case of masonry-like materials as micropolar, second gradient and classical continua, *Acta Mechanica* 225 (1) (2014) 157–177.
- P. Trovalusci, *Discrete to Scale-Dependent Continua for Complex Materials: A Generalized Voigt Approach Using the Virtual Power Equivalence*, Springer International Publishing, Cham, pp. 109–131.
- E. Tadmor, R. Miller, *Modeling Materials: Continuum, Atomistic and Multiscale Techniques*, Cambridge University Press, 2011.
- J. Fan, *Multiscale Analysis of Deformation and Failure of Materials*, Microsystem and Nanotechnology Series (ME20), Wiley, 2011.
- R. Ansari, A. Shahabodini, H. Rouhi, Prediction of the biaxial buckling and vibration behavior of graphene via a nonlocal atomistic-based plate theory, *Compos. Struct.* 95 (2013) 88–94.
- M. Al-Kharusi, K. Alzabedeh, T. Pervez, An atomistic-based continuum modeling for evaluation of effective elastic properties of single-walled carbon nanotubes, *J. Nanomater.* 8641954 (2016) 13pages.
- V. Baudet, M. Beuve, F. Jaillet, B. Shariat, F. Zara, New mass-spring system integrating elasticity parameters in 2d, 2007.
- P. Suryawanshi, A. Gupta, A novel mass spring model topology for modeling of linear isotropic homogenous materials, in: *Proceedings of the ASME International Mechanical Engineering Congress and Exposition*, 2015, p. 8pages.

- 400 [26] A.C. Eringen, On differential equations of nonlocal elasticity and solutions of
401 screw dislocation and surface waves, *J. Appl. Phys.* 54 (9) (1983) 4703–4710. 407
- 402 [27] E. Benvenuti, A. Simone, One-dimensional nonlocal and gradient elasticity:
403 closed-form solution and size effect, *Mech. Res. Commun.* 48 (2013) 46–51. 408
- 404 [28] S. Ghosh, V. Sundararaghavan, A.M. Waas, Construction of multi-dimensional
405 isotropic kernels for nonlocal elasticity based on phonon dispersion data, *Int.*
406 *J. Solids Struct.* 51 (2) (2014) 392–401. 409
- [29] A.A. Pisano, A. Sofi, P. Fuschi, Finite element solutions for nonhomogeneous
nonlocal elastic problems, *Mech. Res. Commun.* 36 (7) (2009) 755–761. 410
- [30] A. Pisano, A. Sofi, P. Fuschi, Nonlocal integral elasticity: 2d finite element based
solutions, *Int. J. Solids Struct.* 46 (21) (2009) 3836–3849. 411
- [31] P. Fuschi, A. Pisano, D. De Domenico, Plane stress problems in nonlocal elas-
ticity: finite element solutions with a strain-difference-based formulation, *J.*
Math. Anal. Appl. 431 (2) (2015) 714–736. 412
413